Structural Engineering and Mechanics, Vol. 44, No. 2 (2012) 179-196
DOI: http://dx.doi.org/10.12989/sem.2012.44.2.179

An eigenspace projection clustering method for structural damage detection

Jun-hua Zhu[1,2], Ling Yu*[1,3] and Li-li Yu[1,4]

[1]*MOE Key Lab of Disaster Forecast and Control in Engineering, Jinan University, Guangzhou, 510632, P. R. China*
[2]*China Electronic Product Reliability and Environmental Testing Research Institute, Guangzhou, 510610, P. R. China*
[3]*Department of Mechanics and Civil Engineering, Jinan University, Guangzhou, 510632, P. R. China*
[4]*School of Materials Science and Engineering, Hebei University of Technology, Tianjin 300130, P. R. China*

(Received February 1, 2011, Revised June 10, 2012, Accepted September 28, 2012)

Abstract. An eigenspace projection clustering method is proposed for structural damage detection by combining projection algorithm and fuzzy clustering technique. The integrated procedure includes data selection, data normalization, projection, damage feature extraction, and clustering algorithm to structural damage assessment. The frequency response functions (FRFs) of the healthy and the damaged structure are used as initial data, median values of the projections are considered as damage features, and the fuzzy c-means (FCM) algorithm are used to categorize these features. The performance of the proposed method has been validated using a three-story frame structure built and tested by Los Alamos National Laboratory, USA. Two projection algorithms, namely principal component analysis (PCA) and kernel principal component analysis (KPCA), are compared for better extraction of damage features, further six kinds of distances adopted in FCM process are studied and discussed. The illustrated results reveal that the distance selection depends on the distribution of features. For the optimal choice of projections, it is recommended that the Cosine distance is used for the PCA while the Seuclidean distance and the Cityblock distance suitably used for the KPCA. The PCA method is recommended when a large amount of data need to be processed due to its higher correct decisions and less computational costs.

Keywords: structural damage detection; eigenspace projections; fuzzy clustering; principal component analysis; kernel principal component analysis

1. Introduction

Structural Health Monitoring (SHM) is a fast-developing, interdisciplinary field of research due to the fact that SHM is heavily stimulated by the engineering problems of maintenance and safe operation of technical infrastructure (Sohn *et al.* 2003, Alvandi and Cremona 2006, Farrar and Worden 2007, Koiakowski 2007, Yan *et al.* 2007, Gul and Catbas 2009, Nguyen and Golinval 2010, Yu and Xu 2011). One of core problems of SHM is the damage identification, which can be divided into five levels (Rytter 1993): 1) detection of damage existence; 2) localization of damage; 3)

*Corresponding author, Professor, E-mail: lyu1997@163.com

identification of damage type; 4) quantification of damage extent; and 5) damage prognosis. The first level, also the lowest level of detection, is to ascertain if damage is present or not based on measured dynamic characteristics of a structure to be monitored (Sohn *et al.* 2003, Sohn 2007), which is the most fundamental issue in the SHM field (Worden *et al.* 2000).

The process of SHM can be considered as one of statistical pattern recognition problems (Farrar *et al.* 2000). Therefore, many algorithms in pattern recognition fields can be applied to solve the SHM problems (Farrar and Worden 2007). Generally speaking, in order to distinguish between the normal condition of the structure and the damaged conditions, one must at least answer two questions: 1) How to extract the features that are insensitive to environmental changes but sensitive to damage from the responses? 2) How to distinguish the damaged and non-damaged state based on the features extracted. These questions are corresponding to the last two portions mentioned by Farrar *et al.* (2000).

The first one is how to extract the damage sensitivity features. In last decades, the most common features used in vibration-based damage detection are the modal parameters, such as the natural frequency, modal shape, and their derivatives, but these features are insensitivity to slight damages, and modal identification can be a time-consuming task and the curve fitting process itself always adds some unavoidable errors. Therefore, the direct use of measured raw data for damage detection (e.g., frequency response functions - FRFs) may represent in most cases a considerable advantage. The measured raw data must be compressed without losing much useful information before performing the damage detection, due to the more redundant information and the less noise immunity. Principal component analysis (PCA) is a well-known tool for feature extraction and dimensionality reduction, which has been widely applied to the damage detection (Zang and Imregun 2001, da Silva *et al.* 2008, Oh and Sohn 2009, Trendafilova *et al.* 2008). However, the PCA mostly are taken as data compression tool and rarely used to directly extract the damage features of structures (Yu *et al.* 2010). This study suggests another use of PCA, which does not reduce the dimension of the FRF data, but project the raw FRF data on the eigenvectors space of covariance of the raw FRF data in reference state. The median values of all their projections are considered as the damage-sensitive features as described by the authors (Yu *et al.* 2010).

In further recognition stage, another question is how to find a critical threshold value that can distinguish undamaged and damaged condition. There are many approaches to determine the critical values, such as statistical process control methods (Fugate *et al.* 2001), Monte Carlo method (Worden *et al.* 2000), fuzzy clustering (da Silva *et al.* 2008), sequential probability ratio test (Oh and Sohn 2009) etc. The statistical process control methods referred to as control chart (e.g., X-bar, S control chart) were used to monitor the mean, the variance or some other function of the features, and the control limits were determined under certain confidence by assuming the distribution of the features to be the normal distribution (Fugate *et al.* 2001). Monte Carlo method means large computation cost. The sequential probability ratio test is based on the premise that damage will increase a standard deviation of the residual error beyond a specified threshold (Oh and Sohn 2009). Fuzzy clustering can categorize the features into two groups, damaged and undamaged states, without using a specified threshold value (da Silva *et al.* 2008). Also other simple discriminant analysis (Trendafilova *et al.* 2008) may be used to classify the features. Here, fuzzy clustering algorithm is used for the recognition objective since the features developed there do not exhibit the property of normal distributions.

In this paper, we present an integrated procedure for damage detection, which combines the data normalization, projection algorithm, and fuzzy clustering techniques. The effectiveness of the

method is evaluated by using an experimental data of three-story frame structure built and tested by Los Alamos National Laboratory, USA. Further, two projection algorithms and six kinds of distances used in the fuzzy c-means (FCM) algorithm are compared and discussed.

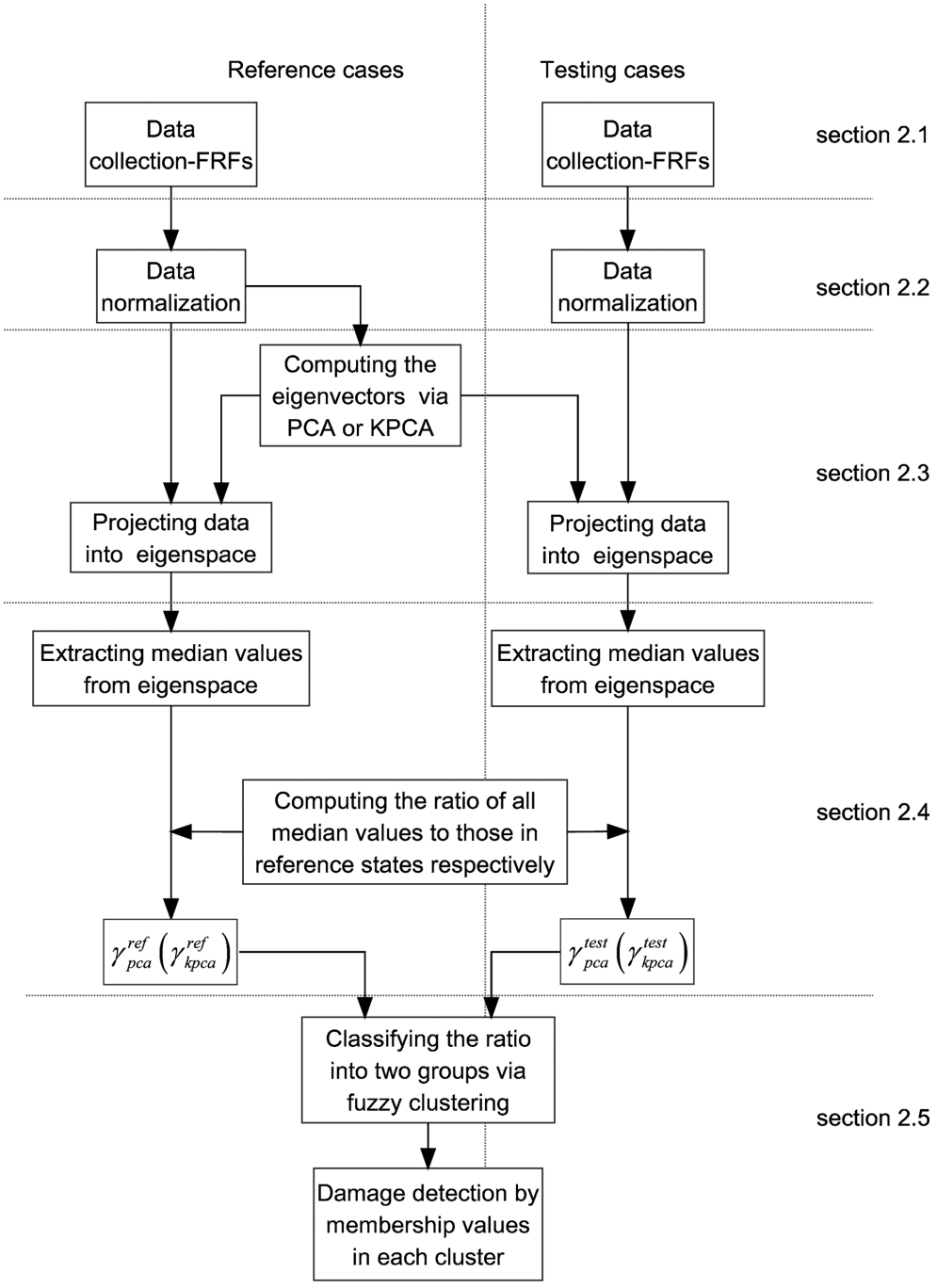

Fig. 1 Damage detection diagram

2. Background of method

The integrated procedure for damage detection are summarized into the diagram in Fig. 1, which can be divided into five steps, i.e., data collection, data normalization, projection, data reduction, and clustering. In this section, the five steps are described as follows.

2.1 Data collection on frequency response functions (FRFs)

The basic premise of vibration-based damage detection is that damage will alter the modal parameters of a structure, which will in turn reflect in the responses of the structure. It has been widely considered that using directly FRFs has more advantages than using indirectly modal parameters in damage detection process, due to the more raw information of FRFs. Thus, in this paper, the FRF data are considered as the initial data.

Assuming a structure under investigation can be modeled as an n-DOF finite element model. In the frequency domain the dynamic equation can be expressed in the form

$$(-\mathbf{M}\omega^2 + \mathbf{C}j\omega + \mathbf{K})\mathbf{X}(\omega) = \mathbf{F}(\omega) \tag{1}$$

where **M**, **C** and **K** are the mass, damping and stiffness matrices respectively, and are symmetric. $\mathbf{X}(\omega)$ and $\mathbf{F}(\omega)$ are the Fourier transforms of the displacement and the forces vectors, respectively, and ω is the excitation frequency. The above equation can be written in terms of FRFs, in the following form

$$\mathbf{X}(\omega) = \mathbf{H}(\omega)\mathbf{F}(\omega) \tag{2}$$

where $\mathbf{H}(\omega)$ is the FRF defined as follows

$$\mathbf{H}(\omega) = (-\mathbf{M}\omega^2 + \mathbf{C}j\omega + \mathbf{K})^{-1} \tag{3}$$

The response of the structure to a harmonic load can be expressed as

$$H_{ij}(\omega) = \sum_{k=1}^{n} \frac{\varphi_{ik}\varphi_{jk}}{\omega_k^2 - \omega^2 + 2j\xi_k\omega_k\omega} \tag{4}$$

where $H_{ij}(\omega)$ is the displacement FRF of the i-th DOF when subjected to the applied unit force at the j-th DOF. The k-th mode shape, natural frequency and damping ratio are represented as φ_k, ω_k, ξ_k respectively. In Eq. (4), it can be seen that one column of FRFs matrix **H** contains all modal parameters. Thus, in fact, it is enough to measure one column of FRFs for structural modal parameters in damage state.

2.2 FRFs data normalization

Let $\mathbf{h} = [\mathbf{h}_1, \mathbf{h}_2, \ldots, \mathbf{h}_p] \in R^{n\times p}$, $\mathbf{h}_i = [h_i(1), h_i(2), \ldots, h_i(n)]^T$, $i = 1, 2, \ldots, p$, denote amplitudes of FRF data with p spectral lines at all n measurement points. In order to eliminate the effects caused by environmental and operational variations from the measured FRFs, the data standardization

procedure are performed as follows (da Silva *et al.* 2008)

$$\hat{h}_i(k) = \frac{h_i(k) - \overline{h}(k)}{\sigma(k)} \tag{5}$$

$$\overline{h}(k) = \frac{1}{p}\sum_{i=1}^{p} h_i(k) \tag{6}$$

$$\sigma^2(k) = \frac{1}{p-1}\sum_{i=1}^{p} (h_i(k) - \overline{h}(k))^2 \tag{7}$$

where $\overline{h}(k), \sigma^2(k)$ and $\hat{h}_i(k)$ are the mean, variance and standardized version of $h_i(k)$ sequence respectively.

2.3 FRFs data projection

Although the FRFs contain more raw information about a structure, considering the cost of computation and effect of noise, it is impossible to use full-size FRF data in a damage detection process. Thus, some measures must be made, such as data reduction and feature extraction. In this section, two projection algorithms, namely principal component analysis (PCA) and kernel principal component analysis (KPCA), are adopted before extracting the damage features. The basic theory is described as follows.

2.3.1 Principal component analysis

PCA is a powerful technique for feature extraction and data dimensionality reduction. It is mathematically (Jolliffe 2002) defined as an orthogonal transformation of raw data to a new coordinate system such that the greatest variance by any projection of the data comes to lie on the first coordinate (called the first principal component), the second greatest variance on the second coordinate, and so on. PCA is theoretically the optimum transform for given data in least square terms.

According to the distribution characteristic of FRF data, it can be concluded that there are strongly correlation between the FRF data at different measurement points. Using the whole FRFs data is not possible. In this scheme, PCA attempts to extract the features from the original data by a linear orthogonal projection.

The covariance matrix of $\hat{\mathbf{h}}_i$ can be computed by

$$\mathbf{C}_1 = \frac{1}{p-1}\sum_{i=1}^{p} \hat{\mathbf{h}}_i \hat{\mathbf{h}}_i^T \tag{8}$$

Then, the PCA can be performed by solving the eigenvalue problem as following

$$\mathbf{C}_1\mathbf{W} = \mathbf{W}\Sigma \tag{9}$$

where $\Sigma = \text{diag}[s_1, s_2, \ldots, s_n]$, $\mathbf{W} = [\mathbf{w}_1, \mathbf{w}_2, \ldots, \mathbf{w}_n] \in R^{n\times n}$, s_i and $\mathbf{w}_i$ are i-th eigenvalue and corresponding eigenvector, respectively. The k-th principal component of the test sample point $\mathbf{h}^{test}$, which is the standardized version of $\mathbf{h}$ in unknown state, is the projection of $\mathbf{h}^{test}$ on the k-th

eigenvector $\mathbf{w}_k$, which can be computed by

$$\mathbf{Z}_k^{pca}(\mathbf{h}^{test}) = \mathbf{w}_k^T \mathbf{h}^{test} \tag{10}$$

In this paper, the eigenvectors are obtained from the normalized FRF data in reference state, and the test points comes from the normalized FRFs data, either in healthy state or in damage state.

2.3.2 Kernel principal component analysis

KPCA, proposed by Schölkopf (1998), is an extension of PCA using techniques of kernel methods. It also can be derived by extension of least-squares support vector machine (Oh and Sohn 2009, Nguyen and Golinval 2010).

Firstly, the data point are mapped into another feature space

$$\hat{\mathbf{h}}_i \to \psi(\hat{\mathbf{h}}_i) \tag{11}$$

In this space, standard PCA is performed. The covariance matrix $\mathbf{C}_2$ of $\psi(\hat{\mathbf{h}}_i)$ is computed by

$$\mathbf{C}_2 = \frac{1}{p-1}\sum_{i=1}^{p} \psi(\mathbf{h}_i)\psi(\mathbf{h}_i)^T = \frac{1}{p-1}\mathbf{\Phi}\mathbf{\Phi}^T \tag{12}$$

which can be diagonalized with nonnegative eigenvalues satisfying

$$\mathbf{C}_2\mathbf{V} = \mathbf{V}\mathbf{\Lambda} \tag{13}$$

where $\mathbf{\Phi} = [\psi(\hat{\mathbf{h}}_1), \psi(\hat{\mathbf{h}}_2), \ldots, \psi(\hat{\mathbf{h}}_p)] \in R^{n\times p}$, $\mathbf{\Lambda} = \mathrm{diag}[\lambda_1, \lambda_2, \ldots, \lambda_n]$ is a diagonal matrix constructed from the eigenvalues of $\mathbf{C}_2$, $\mathbf{V} = [\mathbf{v}_1, \mathbf{v}_2, \ldots, \mathbf{v}_n] \in R^{n\times n}$ is a matrix composed of the corresponding eigenvectors, each column of $\mathbf{V}$ lies in the span of $\psi(\hat{\mathbf{h}}_i)$ $(i = 1, 2, \ldots, p)$ and can be expressed as (Schölkopf 1998)

$$\mathbf{V} = \left[\sum_{i=1}^{p} a_{i1}\psi(\hat{\mathbf{h}}_i), \sum_{i=1}^{p} a_{i2}\psi(\hat{\mathbf{h}}_i), \ldots, \sum_{i=1}^{p} a_{in}\psi(\hat{\mathbf{h}}_i)\right] = \mathbf{\Phi}\mathbf{A} \tag{14}$$

where $\mathbf{A} \in R^{p\times n}$ is the coefficient matrix, whose ij-th element is a_{ij}. Substituting Eq. (12) and (14) into Eq. (13), multiplying both sides with $\psi(\hat{\mathbf{h}}_i)^T$, and rewriting the expression as another eigenvalue problem

$$\frac{1}{p-1}\mathbf{K}\mathbf{A} = \mathbf{A}\mathbf{\Lambda} \tag{15}$$

$$K_{ij} = \psi(\hat{\mathbf{h}}_i)^T\psi(\hat{\mathbf{h}}_j) = \kappa(\hat{\mathbf{h}}_i, \hat{\mathbf{h}}_j) \tag{16}$$

It can be seen that $\mathbf{\Lambda}$ and $\mathbf{A}$ are the eigenvalues and corresponding eigenvectors matrix of $\mathbf{K}/(p-1) \in R^{p\times p}$. $\mathbf{K}$ is the kernel matrix, whose ij-th element is the inner-product kernel $\kappa(\hat{\mathbf{h}}_i, \hat{\mathbf{h}}_j)$. In this paper, the polynomial kernel $\kappa(\hat{\mathbf{h}}_i, \hat{\mathbf{h}}_j) = (\hat{\mathbf{h}}_i^T\hat{\mathbf{h}}_j + 1)^d$ is utilized. Here d is the degree of polynomial, which is set to be 2. The eigenvectors matrix $\mathbf{V}$ is normalized as $\mathbf{I} = \mathbf{V}^T\mathbf{V}$ while the coefficient matrix $\mathbf{A}$ is normalized and translated into $\mathbf{A}^T\mathbf{A} = \Lambda^{-1}/(p-1)$.

The k-th nonlinear principal component of a test point $\mathbf{h}^{test}$ can be extracted in the form

$$\mathbf{Z}_k^{kpca}(\psi(\mathbf{h}^{test})) = \mathbf{v}_k^T\psi(\mathbf{h}^{test}) = \left(\sum_{i=1}^{p} a_{ik}\psi(\hat{\mathbf{h}}_i)\right)^T \psi(\mathbf{h}^{test}) = \sum_{i=1}^{p} a_{ik}(\psi(\hat{\mathbf{h}}_i)^T\psi(\mathbf{h}^{test})) = \sum_{i=1}^{p} a_{ik}\kappa(\hat{\mathbf{h}}_i, \mathbf{h}^{test}) \quad (17)$$

In summary, the following steps were necessary to compute the principal components (PCs): first, compute the kernel matrix $\mathbf{K}$ defined by Eq. (16); second, compute its eigenvectors $\mathbf{A}$ and normalize them; third, compute projections of a test point onto the eigenvectors by Eq. (17). In fact, the mapping ψ does not need to be computed explicitly since the whole procedures only need kernel matrix $\mathbf{K}$, which can be implicitly obtained.

Care must be taken into consideration regarding the fact that whether $\hat{\mathbf{h}}_i$ has zero-mean in its original space or not, it is not guaranteed to be centered in the feature space. Since centered data is required to perform an effective PCA, the centralized version of $\mathbf{K}$ can be computed by (Schölkopf 1998)

$$\mathbf{K}^* = \mathbf{K}^* - \mathbf{1}_p\mathbf{K} - \mathbf{K}\mathbf{1}_p + \mathbf{1}_p\mathbf{K}\mathbf{1}_p \quad (18)$$

where $\mathbf{1}_p$ denotes a p-by-p matrix for which each element takes value $1/p$.

2.4 Damage sensitivity features extracted from projections

It is impossible to use all projections obtained previously in the damage detection process. Damage sensitivity index should be extracted further from the PCs. Recently, the median values of PCs are proposed in reference (Yu *et al.* 2010), and the results show that it can reflect the structural state. By definition

$$\alpha_k = median(\mathbf{Z}_k^{pca}(\mathbf{h}^{test})) \quad (19)$$

$$\beta_k = median(\mathbf{Z}_k^{kpca}(\mathbf{h}^{test})) \quad (20)$$

$$\gamma_{pca}(k) = \frac{\alpha_k^{test}}{\alpha_k^{ref}} \quad (21)$$

$$\gamma_{kpca}(k) = \frac{\beta_k^{test}}{\beta_k^{ref}} \quad (22)$$

where α_k and β_k denote the median values of the k-th principal component obtained by PCA and by KPCA respectively. The superscripts in Eqs. (21) and (22), i.e. ^{test} and ^{ref}, denote the median values in the testing states and the reference state respectively. If no damage occurred, the damaged index (γ_{pca}, γ_{kpca}) theoretically equal to unity, otherwise, it should be greater or smaller than unity. In fact, the damaged index cannot absolutely equal to unity, even in healthy state, due to the effect of environmental factors. The damage detection can be performed correctively according to the whole features of the damaged index.

2.5 Damage detection using fuzzy clustering

In the previous section, damaged index has been defined, but it is difficult to choose a threshold values that characterize damage. In order to perform the damage detection, fuzzy c-means clustering (FCM) algorithm, which was first presented by Bezdek (1981), and recently applied to SHM problems by da Silva *et al.* (2008), is employed to clarify the features, and supply a fuzzy decision by using the membership of damage index in a cluster. This algorithm is an unsupervised classification algorithm which uses a certain objective function, described in Eq. (23), for iteratively determining the local minima.

$$\min J(C,m) = \sum_{i=1}^{C}\sum_{j=1}^{N} u_{ij}^{m} d_{ij}^{2} \tag{23}$$

$$\mathbf{c}_i = \frac{\sum_{j=1}^{N} u_{ij}^{m}\mathbf{x}_j}{\sum_{j=1}^{N} u_{ij}^{m}} \tag{24}$$

$$d_{ij}^{2} = (\mathbf{x}_j - \mathbf{c}_i)^{T}(\mathbf{x}_j - \mathbf{c}_i) \tag{25}$$

$$u_{ij} = \frac{(d_{ij})^{\frac{-2}{m-1}}}{\sum_{i=1}^{C}(d_{kj})^{\frac{-2}{m-1}}} \tag{26}$$

where C is the total number of clusters, which here is set to be 2 that denote two states, such as the healthy and damaged state in this paper. N is the total number of objects in calibration. u_{ij} is the membership function associated with the j-th object of the i-th cluster, which is updated by using Eq. (26) in each iteration step. The exponent m is a measurement of fuzzy partition. $\mathbf{c}_i$ is the centroid of the i-th cluster, $\mathbf{x}_j$ is j-th object of data set to be clustered, which here is set to γ, d_{ij} denotes the distance between j-th object and the centroid of the i-th cluster, here, Euclidean distance is used as Eq. (25) (Matlab 2000).

3. An experimental example for structural damage detection

3.1 Experimental description

To verify the proposed method, an experimental example based on a three-story frame structure (Fig. 2) is used here. The background and time history data are available from the Los Alamos National Laboratory website (http://institute.lanl.gov/ei/). The structure was built of Unistrut columns and aluminum floor plates with two-bolt connections to the brackets on the Unitstrut. Twenty-four piezoelectric single-axis accelerometers ($n = 24$), two per joint, were mounted on the aluminum blocks, eight in each plate. The shaker was attached at Corner D using a stinger

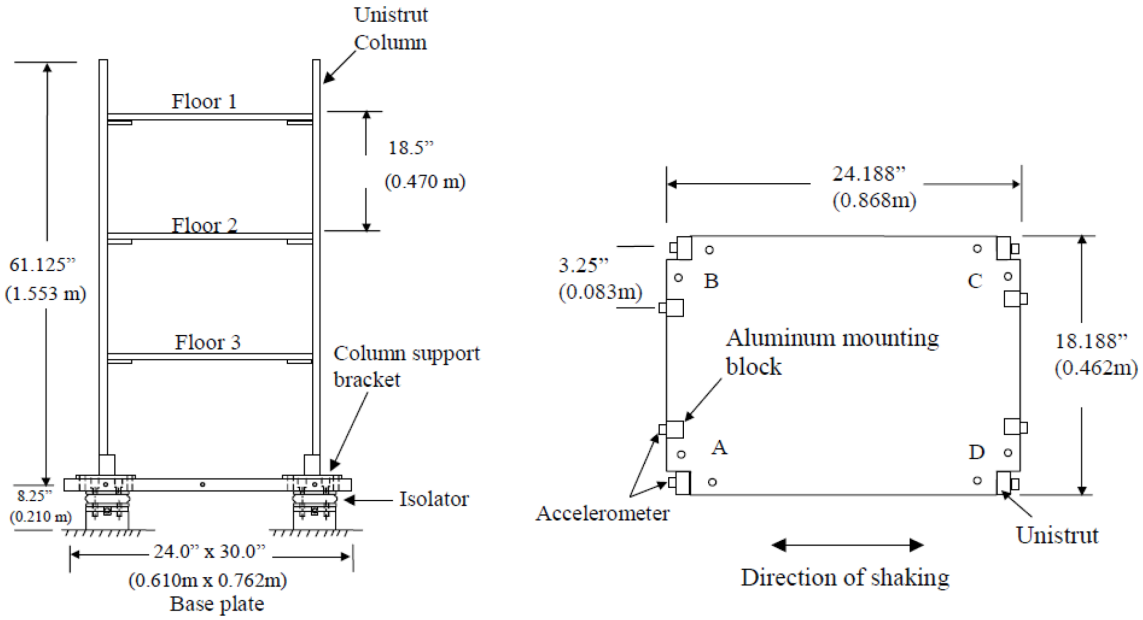

Fig. 2 Three-story frame structure

connected to a tapped hole at the mid-height of the base plate and a force transducer is also mounted between the stinger and the base plate to measure the excitation input.

3.2 Experimental cases

The experimental investigation includes a number of healthy states (HS) and damaged states (DS) with single and multiple damage locations and varying damage levels. The following cases are considered.

HS1: Reference state;
DS1: Damage introduced to location 1C, including two damage levels (DB0 and DBB);
HS2: Healthy state recovered from DS1;
DS2: Damage introduced to location 3A, including two damage levels (DB0 and DBB);
HS3: Healthy state recovered from DS2;
DS3: Damage introduced to location 1C and 3A, including two damage levels (DB0 and DBB);
HS4: Healthy state recovered from DS3;
DS4: Damage introduced to location 1C, including three damage levels (D05, D10 and DHT);
HS5: Healthy state recovered from DS4.
The damage levels include DB0, DBB, D05, D10 and DHT, which mean
DB0: Bolts were removed between the bracket and the plate;
DBB: Bracket was completely removed;
D05: Torque value of 5 ft.Lbs was left on the bolts;
D10: Torque value of 10 ft.Lbs was left on the bolts;
DHT: Hand tight torque was left on the bolts.

Table 1 List of known state (reference state)

Case	Structural condition	damage location	damage extent	Excitation level (V)
1	Health State (HS1)	-	D00	2

Table 2 List of unknown states

Case	Structural State	Damage Location	Damage extent	Excitation Level (V)	Case	Structural State	Damage Location	Damage extent	Excitation Level (V)
2	Healthy States (HS1)	-	D00	2	32	Damaged States (DS3)	1C and 3A	DB0	2
3		-	D00	2	33		1C and 3A	DB0	5
4		-	D00	5	34		1C and 3A	DB0	8
5		-	D00	5	35		1C and 3A	DBB	2
6		-	D00	8	36		1C and 3A	DBB	5
7		-	D00	8	37		1C and 3A	DBB	8
8	Damaged States (DS1)	1C	DB0	2	38	Healthy States (HS4)	-	D00	2
9		1C	DB0	5	39		-	D00	2
10		1C	DB0	8	40		-	D00	5
11		1C	DBB	2	41		-	D00	5
12		1C	DBB	5	42		-	D00	8
13		1C	DBB	8	43		-	D00	8
14	Healthy States (HS2)	-	D00	2	44	Damaged States (DS4)	1C	D05	8
15		-	D00	2	45		1C	D05	8
16		-	D00	5	46		1C	D10	8
17		-	D00	5	47		1C	D10	8
18		-	D00	8	48		1C	DHT	8
19		-	D00	8	49		1C	DHT	8
20	Damaged States (DS2)	3A	DB0	2	50	Healthy States (HS5)	-	D00	2
21		3A	DB0	5	51		-	D00	2
22		3A	DB0	8	52		-	D00	5
23		3A	DBB	2	53		-	D00	5
24		3A	DBB	5	54		-	D00	8
25		3A	DBB	8	55		-	D00	8
26	Healthy States (HS3)	-	D00	2					
27		-	D00	2					
28		-	D00	5					
29		-	D00	5					
30		-	D00	8					
31		-	D00	8					

Notes: D00 indicates no damage occurs, DB0 indicates that the bolts were removed between the bracket and the plate, DBB indicates the bracket was completely removed, DHT indicates the bolts were left in at a hand tight torque, and D05/D10 indicate that a torque value of 5 or 10 ft. Lbs. was left on the bolts.

Random shaker excitation was applied to the base, and the responses were sampled at 1600 Hz with each signal consisting of 8192 points. The FRFs were calculated from both the measured force and response signals. In order to reduce the random fluctuation in the estimation of the FRFs, the number of averaging individual time records was selected to be eight as the same setting as the ref (Zang *et al.* 2003). The final FRF was produced with 512 spectrum lines ($p = 512$). The reference state is chosen from the healthy state (HS1) arbitrarily, supposed to be the FRFs using the excitation levels of 2V as listed in Table 1, and the configurations of all test cases are listed in Table 2. It should be noted that the FRFs data used in Case 1 are different from those used in Cases 2-7.

3.3 Results and discussions

Fig. 3 plots the FRF curves in the same condition with different excitation levels, where the figure legend "Case6: HS1-D00-8-2" denotes Case 6 corresponding to the HS1 state with D00 damage extent and 8V excitation level as shown in Table 2, the last digit 2 is the set number. D00 indicates no damage occurs. Other legends in the following figures can be recognized similarly. It can be seen from Fig. 3 that data normalization is very effective to remove the effect of the excitation levels, which cause the increasing or decreasing of amplitude in FRF curves.

The median values of PCs in different states are compared in Fig. 4. The PCA can give 24 eigenvectors corresponding to 24 non-zero eigenvalues, however, the KPCA can supply 415 non-zero eigenvalues, which result in 24 and 415 median values for the two projection algorithms, PCA and KPCA, respectively. It can be seen that the last median values of PCs are sensitive to damage, whether using normal PCA or KPCA. This is because damage can only induce changes in FRF

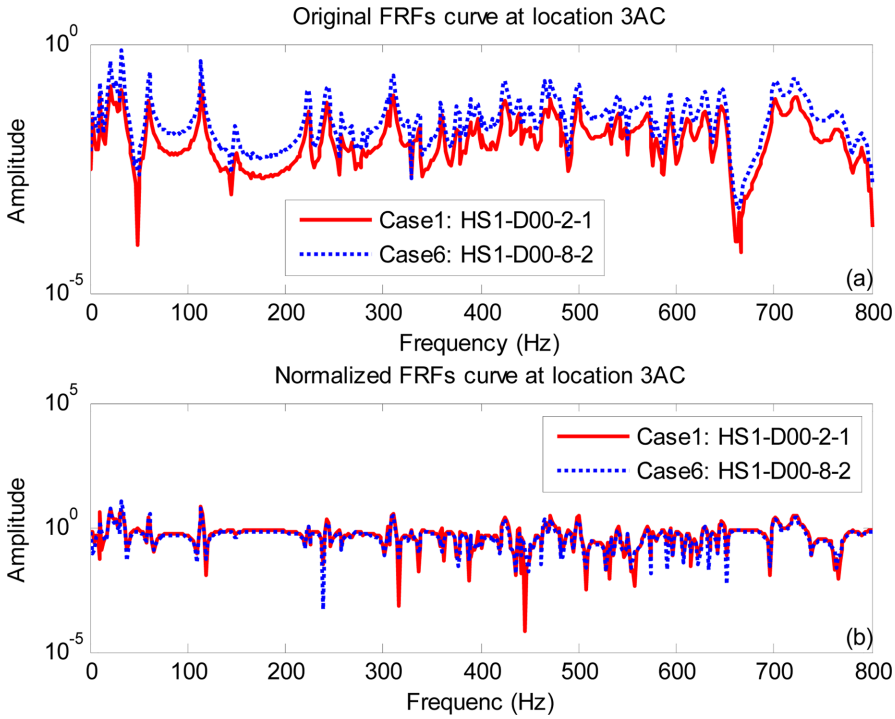

Fig. 3 Comparison on FRF curves before and after normalization

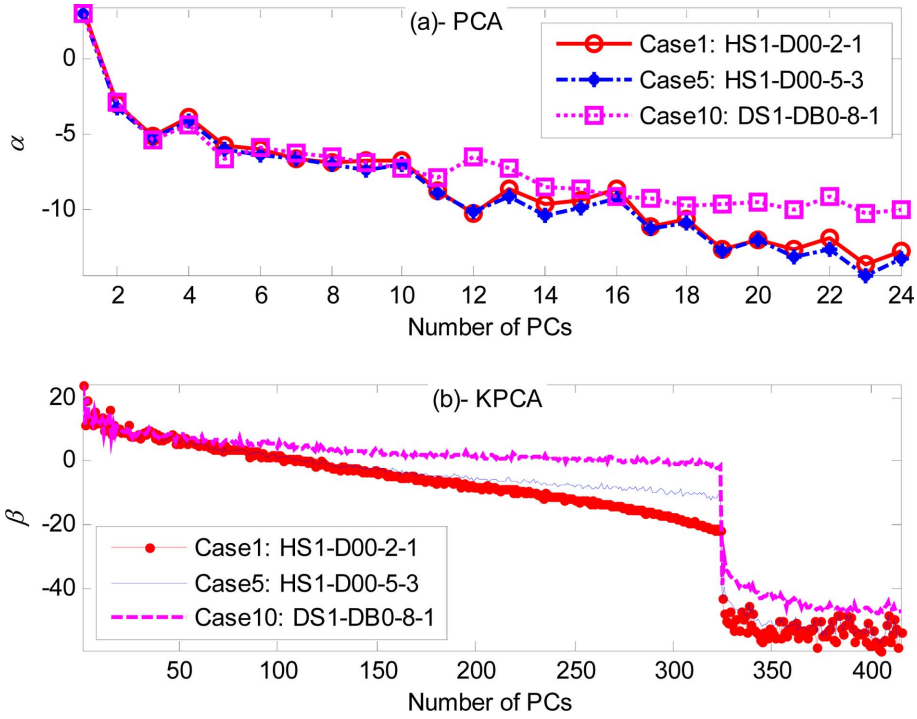

Fig. 4 Comparison on median values of PCs in different states

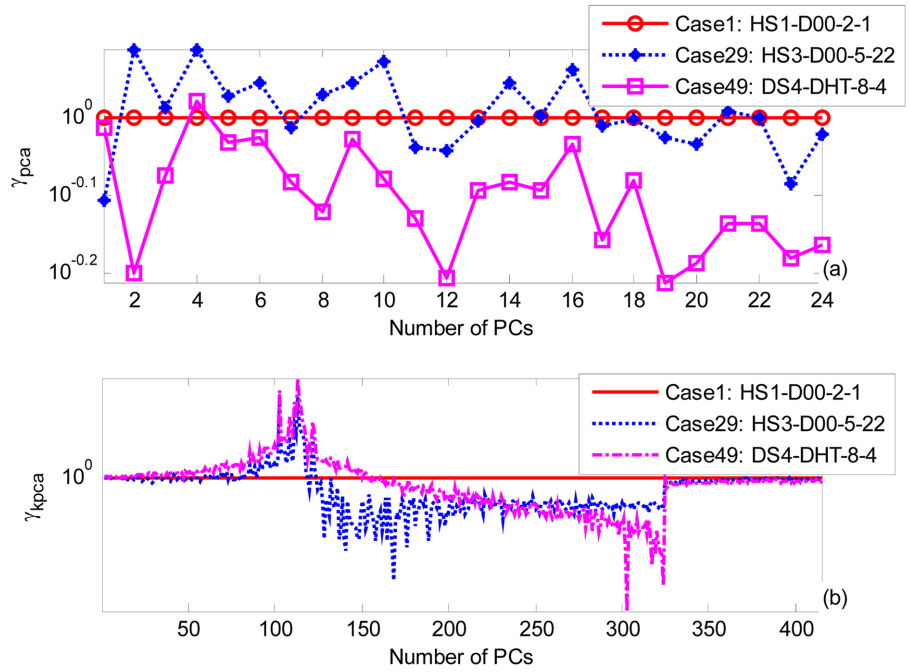

Fig. 5 Feature indexes extracted by PCA and KPCA

locally, not entirely. If the median values of the first few PCs vary remarkably, which indicates serious damage arises, but it does not mean that changes of the last median values suggest damaged occurred due to the effect of noise.

Then, how to detect damage occurred in structure from the variety of the median values? In this paper, the fuzzy c-means clustering algorithm is used to supply a fuzzy decision by finding the hidden patterns in damaged structure. The damage indexes are computed by Eqs. (21) and (22) respectively, some of them are plotted in Fig. 5. From Fig. 5(a), it can be seen clearly that the damage index in Case 29 (healthy state) fluctuates around unity in Case 1 (reference state) and that in Case 49 (damaged state) takes an offset. Fig. 5(b) is the damage index obtained by KPCA, it also shows a distinct pattern between Case 29 (healthy state) and Case 49 (damaged state), especially at the middle section, where the damage index in Case 29 (healthy state) exhibits an excursion pattern while that in Case 49 (damage state) shows an rotation pattern.

Further, the damage index computed with PCA and KPCA were taken as the input of FCM respectively, in which the cluster number $C = 2$ and the exponent $m = 1.5$. Fig. 6 and Fig. 7 plot the centroid of clusters derived from these damage indexes respectively, each centroid of clusters represents the healthy or damaged pattern. It can be seen that there exists clearly different patterns in healthy and damaged structure.

The membership values of each case in each cluster are presented in Fig. 8 and Fig. 9, it can be seen that all undamaged cases were classified well when using PCA. There were a false-positive in Case 43 when using KPCA. For the damaged cases, Figs. 8 and 9 show that the KPCA result is better than the PCA result, because there were about 88.9% correct decisions for the KPCA with 5 false-negatives in Cases 21, 22, 44, 46 and 47, whereas there are about 87% correct decisions for the PCA with 7 false-negatives in Cases 21, 22, 24, 25, 44, 46 and 47.

In the FCM process, two parameters play an important role in the clustering results. One is the exponent m, in general, the higher the exponent, the more vague the boundary between different

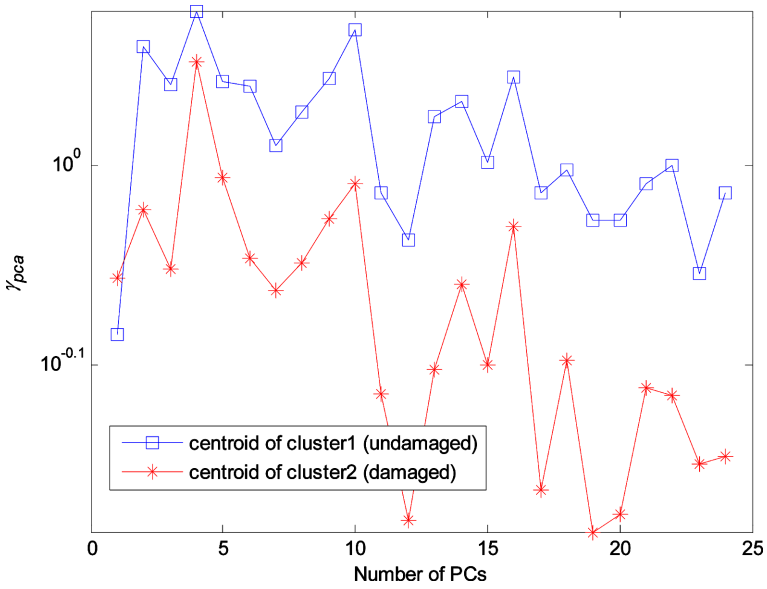

Fig. 6 Centroid of clusters derived from feature index by PCA

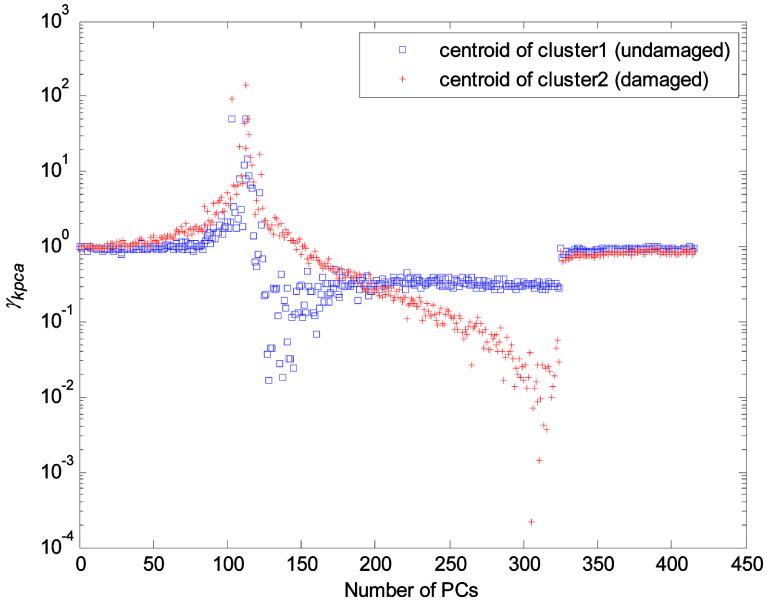

Fig. 7 Centroid of clusters derived from feature index by KPCA

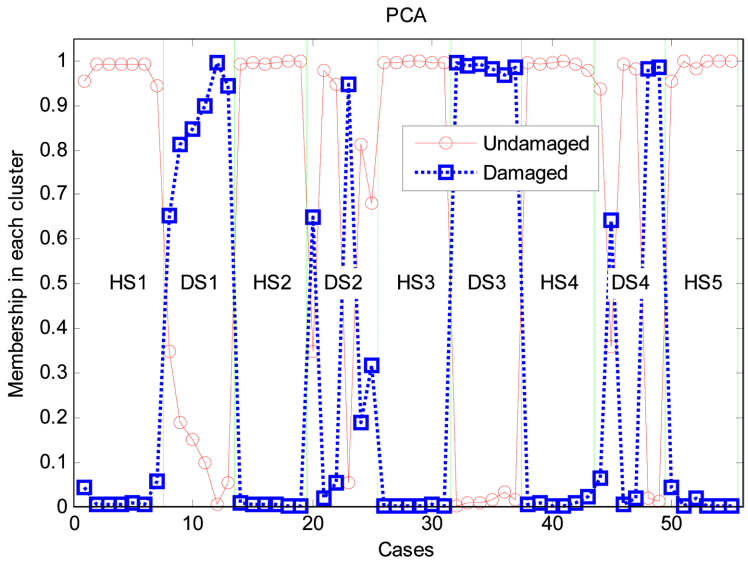

Fig. 8 Membership of each case in each cluster (PCA)

cluster. The exponent is always greater than unity, m = 1.5 is set here. Another one is the distance d_{ij}, the results mentioned above were obtained by using Euclidean distance in Eq. (25). In order to investigate the effect of different distance on the results, we adopt another five distances (Matlab 2000) as in Table 3 instead of Euclidean distance. The results of PCA and KPCA were plotted in Fig. 10 and Fig. 11 respectively.

It should be noted that only the membership in damaged cluster were plotted in Fig. 10 and

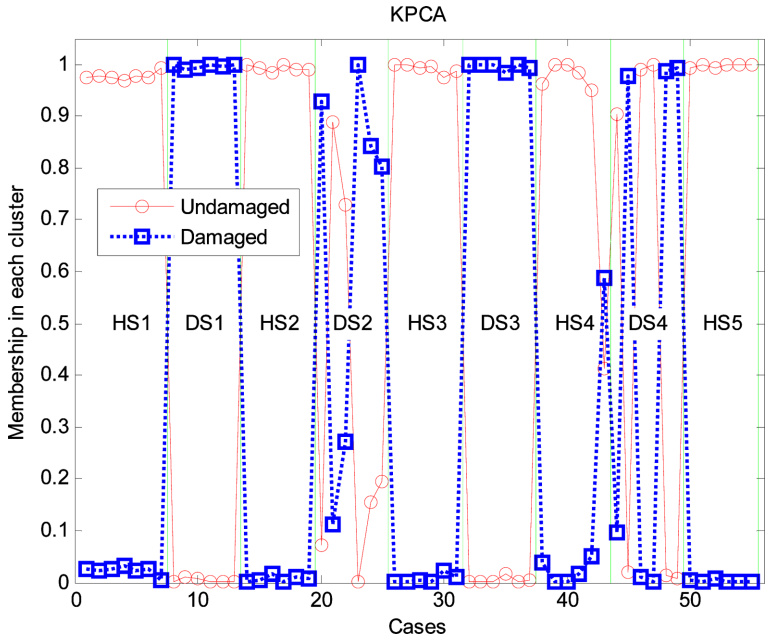

Fig. 9 Membership of each case in each cluster (KPCA)

Table 3 Various distances

Distance	Equation	Notes
Seuclidean	$d_{ij}^2 = (x_j - center_i)^T S^{-1}(x_j - center_i)$	Where S is a diagonal matrix whose j-th diagonal element is s^2, where s is the vector x_j of standard deviations.
Cityblock	$d_{ij} = \sum_k \lvert x_{jk} - center_{ik} \rvert$	The city block distance is a special case of the Minkowski metric, where $p = 1$.
Minkowski	$d_{ij} = \sqrt[p]{\sum_k \lvert x_{jk} - center_{ik} \rvert^p}$	For the special case of $p = 1$, the Minkowski metric gives the City Block metric, for the special case of $p = 2$, the Minkowski metric gives the Euclidean distance, and for the special case of $p = \infty$, the Minkowski metric gives the Chebychev distance. In this paper, $p = 3$ is used.
Chebychev	$d_{ij} = \max_j\{\lvert x_{jk} - center_{ik} \rvert\}$	The Chebychev distance is a special case of the Minkowski metric, where $p = \infty$.
Cosine	$d_{ij} = 1 - \frac{x_j^T center_i}{\sqrt{(x_j^T x_j)(center_i^T center_i)}}$	

Fig. 11, as the summation of membership of each case in two clusters always equal to unity. The closer the membership in damaged cluster is to unity, the higher the probability of damage, and vice versa. From Fig. 10, it can be seen that there are no evident improvement in the results of all cases using various distances except those using Cosine distance, which classifies the Cases 21, 22, 24 and 25 correctly, and increases correct decisions of the PCA to be 92.6%. Fig. 11 shows that the poor results for the KPCA may be obtained when using Cosine distance for damaged cases, the

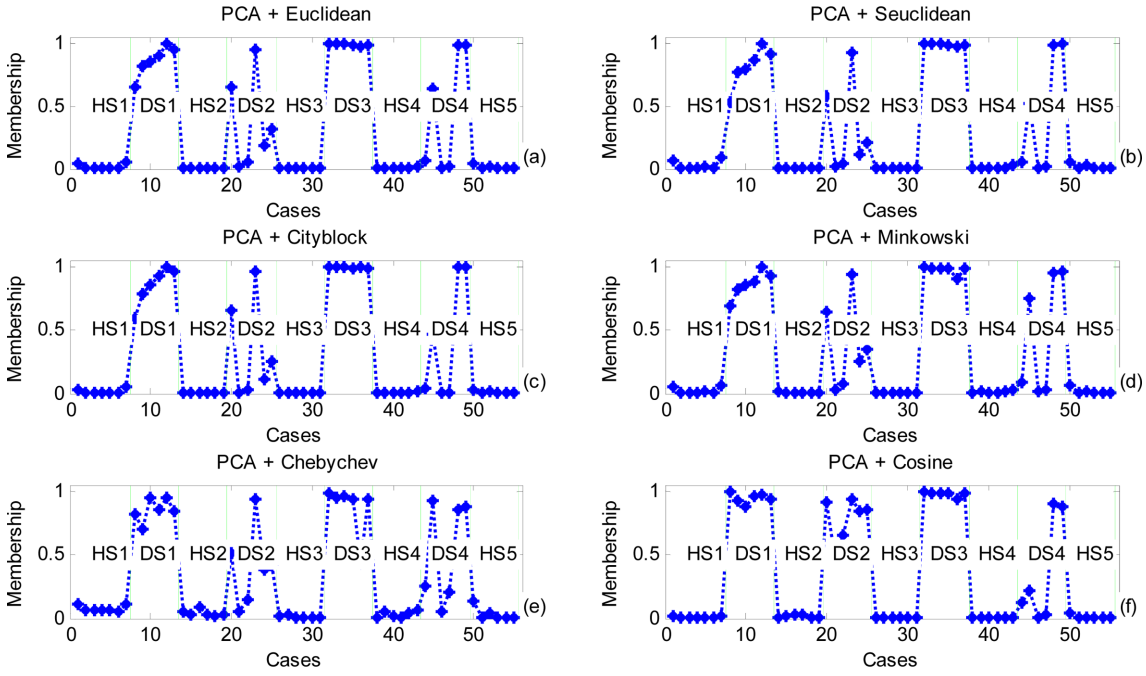

Fig. 10 Membership of each case in damaged cluster by PCA

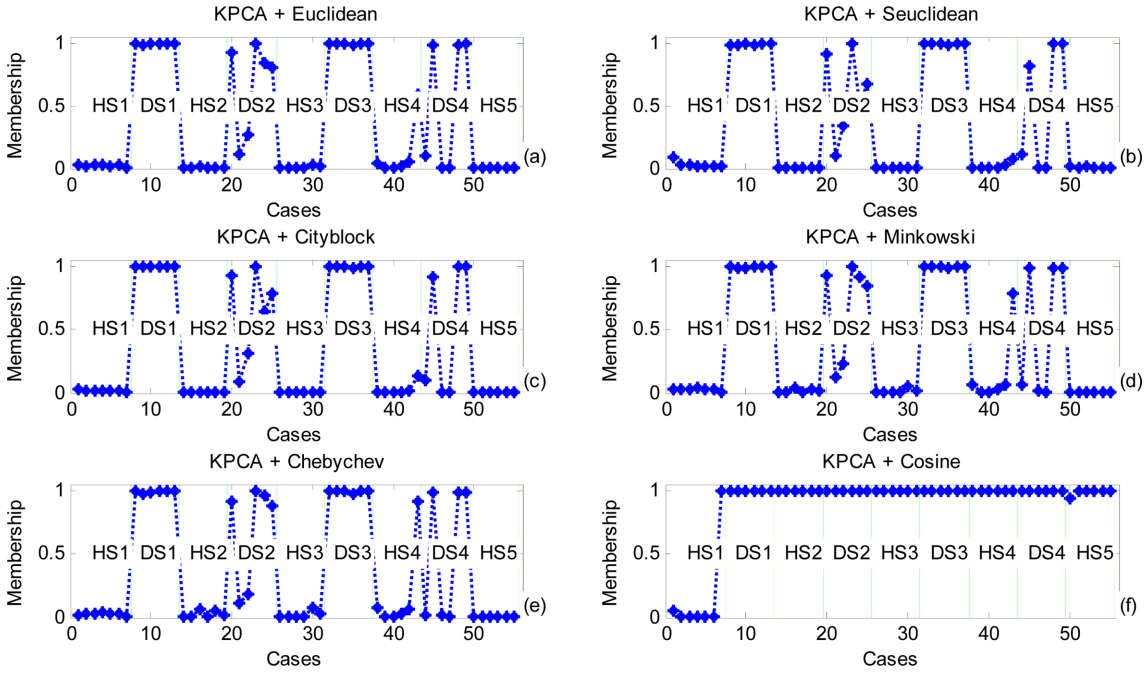

Fig. 11 Membership of each case in damaged cluster by KPCA

results of each case using all distances except Cosine distance, are similar to each other. However, there were no false-positive when using Seucildean distance and Cityblock distance with 5 false-negatives in Cases 21, 22, 44, 46, and 47. The correct decision is up to 90.7%.

In Cases 21, 22, 24 and 25 corresponding to DS2, when Euclidean distance was used for PCA and any of distances used for KPCA, there was lower correct decisions, which is consistent with the results in the ref (da Silva *et al.* 2008). But when Cosine distance was used for PCA, these cases can be classified correctly. However, in Cases 44, 46 and 47 corresponding to DS4, both two algorithms failed to detect damage when any of distances was used for PCA, which may be due to the slight damage.

4. Conclusions

An eigenspace projection clustering method is proposed in this paper for structural damage detection on the basis of measured frequency response functions (FRFs). An experimental example of three-story frame structure validated its effectiveness, further two projection algorithms, namely principal component analysis (PCA) and kernel principal component analysis (KPCA), and six distances in the fuzzy c-means (FCM) algorithm were compared respectively, some conclusions can be made as follows:

(i) Before performing data projection, data normalization is very necessary for eliminate the environmental and operational effects.

(ii) By comparing the results of two projection algorithms, i.e. PCA and KPCA, KPCA were found to be slightly better than PCA when using any distance except Cosine distance in the FCM process. However, when using Cosine distance, the correct decision for PCA increases to be 92.6%. Considering the computational costs induced by KPCA, PCA is better than KPCA.

(iii) Which distance should be chosen in damaged detection process? The results show that it should be based on the distribution of features corresponding to γ in this paper. For the special case, it is recommended that the Cosine distance is used for PCA while the Seuclidean distance and the Cityblock distance is suitably used for KPCA.

(iv) This integrated method contains five steps, i.e., data collection, data normalization, projection, data reduction, and clustering, which is associated with each other. The experimental example shows that it can give the more robust damage detection results, compared with the existing approach proposed by da Silva (da Silva *et al.* 2008). It has many desirable features for utilization in real-world structures, as for instance: it needs only one sample in healthy state to be as the reference data; damage detection procedure is conducted in an unsupervised learning mode, and doesn't need a predefined threshold value. However, there still exist some issues needed to be investigated, such as the effect of kernel function, nonlinearity damage detection and damage localization and quantification etc. Further research is being conducted dealing with all these issues.

Acknowledgments

The authors would like to gratefully acknowledge the joint support of the National Natural Science Foundation of China (50978123, 51278226 and 11032005), Guangdong Natural Science Foundation (10151063201000022) and the Fundamental Research Funds for the Central Universities

(21609601). The authors are also grateful to LANL because the measured data of the three story frame structure can be downloaded freely from the LANL website.

References

Alvandi, A. and Cremona, C. (2006), "Assessment of vibration-based damage identification techniques", *J. Sound Vib.*, **292**, 179-202.

Bezdek, J.C. (1981), *Pattern Recognition with Fuzzy Objective Function Algorithm*, Plenum Press, NY.

da Silva, S., Dias Júnior, M., Lopes Junior, V. and Brennan, M.J. (2008), "Structural damage detection by fuzzy clustering", *Mech. Syst. Signal Pr.*, **22**, 1636-1649.

Farrar, C.R., Duffey, T.A., Doebling, S.W. and Nix, D.A. (2000), "A statistical pattern recognition paradigm for vibration-based structural health monitoring", *Proceedings of 2nd International Workshop on Structural Health Monitoring*, Stanford, CA, USA.

Farrar, C.R. and Worden, K. (2007), "An introduction to structural health monitoring", *Philos. Trans. Royal Soc. A*, **365**, 303-315.

Fugate, M.L., Sohn, H. and Farrar, C.R. (2001), "Vibration-based damage detection using statistical process control", *Mech. Syst. Signal Pr.*, **15**, 707-721.

Gul, M. and Catbas, F.N. (2009), "Statistical pattern recognition for Structural Health Monitoring using time series modeling: Theory and experimental verifications", *Mech. Syst. Signal Pr.*, **23**, 2192-2204.

Jolliffe, I.T. (2002), *Principal Component Analysis*, Springer, NY.

Koiakowski, P. (2007), "Structural health monitoring–a review with the emphasis on low-frequency methods", *Eng. Tran.*, **55**, 239-275.

MATLAB (2000), *Toolbox User's Guide*, http://www.mathworks.com/products/, The MathWorks, Inc..

Nguyen, V.H. and Golinval, J.C. (2010), "Fault detection based on Kernel Principal Component Analysis", *Eng. Struct.*, **32**, 3683-3691.

Oh, C.K. and Sohn, H. (2009), "Damage diagnosis under environmental and operational variations using unsupervised support vector machine", *J. Sound Vib.*, **325**, 224-239.

Rytter, A. (1993), "Vibration based inspection of civil engineering structures", Aalborg University, Denmark.

Schölkopf, B., Smola, A. and Müller, K.R. (1998), "Nonlinear component analysis as a kernel eigenvalue problem", *Neural Comput.*, **10**, 1299-1319.

Sohn, H. (2007), "Effects of environmental and operational variability on structural health monitoring", *Philos. Trans. Royal Soc. A*, **365**, 539-560.

Sohn, H., Farrar, C.R. and Hemez, F.M. (2003), "A review of structural health monitoring literature: 1996–2001", LA-13976-MS, Los Alamos National Laboratory Report, New Mexico.

Trendafilova, I., Cartmell, M.P. and Ostachowicz, W. (2008), "Vibration-based damage detection in an aircraft wing scaled model using principal component analysis and pattern recognition", *J. Sound Vib.*, **313**, 560-566.

Worden, K., Manson, G. and Fieller, N.R.J. (2000), "Damage detection using outlier analysis", *J. Sound Vib.*, **229**, 647-667.

Worden, K. and Manson, G. (2007), "The application of machine learning to structural health monitoring", *Philos. Trans. Royal Soc. A*, **365**, 515-537.

Yan, Y., Cheng, L., Wu, Z. and Yam, L. (2007), "Development in vibration-based structural damage detection technique", *Mech. Syst. Signal Pr.*, **21**, 2198-2211.

Yu, L. and Xu, P. (2011), "Structural health monitoring based on continuous ACO method", *Microelectron. Reliab.*, **51**, 270-278.

Yu, L., Zhu, J.H. and Chen, L.J. (2010), "Parametric study on PCA-based algorithm for structural health monitoring", *Proceedings of IEEE Prognostics and Health Management Conference*, Macau University, Macau, January.

Zang, C., Friswell, M.I. and Imregun, M. (2003), "Structural health monitoring and damage assessment using measured FRFs from multiple sensors, part I: The indicator of correlation criteria", *Proceedings of 5th International Conference on Damage Assessment of Structures*, Southampton, England.

Zang, C. and Imregun, M. (2001), "Structural damage detection using artificial neural networks and measured FRF data reduced via principal component projection", *J. Sound Vib.*, **242**, 813-827.